

Ultrasonic-phase-velocity measurements in electron-irradiated quartz

A. Vanelstraete and C. Laermans

Laboratorium voor Vaste Stof- en Hoge Druk-Fysika, Departement Natuurkunde, Katholieke Universiteit Leuven, Celestijnenlaan 200D, B-3030 Leuven, Belgium

(Received 8 July 1988)

Precision measurements of the ultrasonic velocity change as a function of temperature were carried out in electron-irradiated quartz (dose = 1.0×10^{20} e/cm², $E = 3$ MeV) for two frequencies: 648 and 480 MHz. Between 0.33 and 2 K, a frequency-independent logarithmic increase of the velocity is observed. The effect is very small, but clearly indicates the presence of the resonant interaction of tunneling states with phonons. The experiment shows that tunneling states of a two-state nature are present. In addition, the effect of the relaxation process on the velocity is observed and shows that the tunneling states are of the same nature as in glasses. A comparison with neutron-irradiated quartz indicates that similar tunneling states are induced by electrons and neutrons, in spite of the different disordering processes. It is suggested that the electron-induced Frenkel pairs provide the necessary freedom for rearrangements and rotations of the tetrahedra, which can be at the origin of the tunneling states.

At low temperatures, amorphous solids exhibit dynamical properties which are totally different from those in crystals.¹ A phenomenological model which can describe all data so far obtained, even on glasses of very different structures, assumes the existence of configurational tunneling states (TS),² also more simply described as two-level systems (TLS).³ The microscopic origin of these TS is not yet clear. In search of a model substance, other workers as well as ourselves have shown similar excitations to exist in partly disordered crystals. The excitations have broad spectra in both energy and relaxation time and in some of these disordered crystals these spectra may be changed systematically by varying the amount of disorder. Irradiated quartz is very attractive as a model of the glassy state, as it allows continuous structural variations from the perfectly ordered crystal to the amorphous network disorder. Similar anomalies to those in glasses have been observed in neutron-irradiated quartz⁴⁻⁷ and were also explained by the existence of tunneling states similar in nature to those in vitreous silica.

It is relevant to inquire how much order and what type of disorder is needed to produce these tunneling states in an otherwise perfect crystal. For this study, electron-irradiated quartz is an even more interesting model substance than neutron-irradiated quartz. As compared to neutrons, the use of MeV electrons reduces and simplifies the possible processes of interaction with the structure of the bombarded substance. Electrons, because of their small mass, transfer relatively little energy to the atoms which they hit. This excludes the production of highly disordered regions caused by cascade processes, as is the case for neutron irradiations.

Thermal conductivity⁸ and, recently, ultrasonic attenuation⁹ measurements have given evidence for the existence of TS in electron-irradiated quartz. In the present paper, precision measurements of the temperature-dependent phase velocity of sound show unambiguously

the two-state nature of the excitations, having very low energy. This is the first time that a temperature-dependent change in the velocity has been observed in electron-irradiated quartz at low temperatures. The frequency-independent logarithmic increase of the velocity at the lowest temperatures clearly indicates the resonant interaction of the TS with the phonons. The analysis of the velocity data was performed in the framework of the tunneling model. For comparison, velocity measurements were also carried out in neutron-irradiated quartz and indicate that the tunneling states in electron-irradiated quartz are of a similar nature to those in neutron-irradiated quartz and vitreous silica. The existence of TS in electron-irradiated quartz will be further related with studies of the damage created by electrons in quartz.

An X-cut single crystal of natural Brazilian quartz of high purity was irradiated with 3-MeV electrons up to a dose of 1.0×10^{20} e/cm². Neutron activation analysis showed as impurities in units of $\mu\text{g/g}$:

Al, 12; Cr, 9; Fe, 65; Mn, 0.3; Ti, 17 ;

Co, 0.4; Cu, 22; K, 60; Na, 7.8; V, 0.8 .

The electron irradiation was carried out in a Van de Graaf generator (at Centre d'Etudes Nucléaires-Grenoble) with a flux of $2.6 \mu\text{A}/\text{cm}^2$. The variation of the longitudinal velocity of sound in this sample (E3) was measured at two frequencies, 648 and 480 MHz, in the temperature range 0.33–15 K. For comparison, velocity measurements were also performed in a slightly neutron-irradiated quartz sample (K9), exposed to a fast neutron dose 1.36×10^{18} n/cm² ($E \geq 0.1$ MeV) or 0.85×10^{18} n/cm² ($E \geq 0.3$ MeV). The measurements were performed at 648 MHz. The variation of the ultrasonic velocity was also measured in an unirradiated synthetic quartz sample at 648 MHz. The impurity contents of the unirradiated and neutron-irradiated quartz sample are

given in Ref. 10. Accurate velocity measurements of the order of $\Delta v/v = 10^{-7}$ were possible with a modified pulse interference method.¹¹

In Fig. 1, the variation of the longitudinal velocity of sound in the electron-irradiated quartz specimen (E3) is given as a function of the temperature for the frequencies 648 and 480 MHz. A logarithmic increase of the velocity change which is independent of the frequency is seen below 2 K. It is similar to the behavior in glasses, but about 200 times smaller.¹² This is the first time that this behavior has been measured in electron-irradiated quartz. The velocity increase is very small, but the precision of the present relative velocity measurements, $\Delta v/v$, better than 2×10^{-7} , above 0.5 GHz, has enabled us to observe this effect. It shows the presence of excitations of a two-state nature and of very low energy, also called tunneling states in glasses. This is the result of the resonant interaction between the ultrasonic wave and these tunneling states. The TS in glasses can be described with the tunneling model. For the interaction of the phonons with the TS, the tunneling model distinguishes between two contributions to the dispersion. At very low temperatures ($T \leq 1$ K), the contribution of the resonant interaction between the ultrasonic wave and a TS is dominant in our frequency range. It leads to a logarithmic increase of the velocity with temperature. At higher temperatures, the contribution of the relaxation process also becomes important, resulting in a decrease of the velocity with temperature. The contribution of the resonant interaction to the sound velocity can be derived by using the Kramers-Kronig relation between sound absorption and sound dispersion, and is^{2,3}

$$\frac{\Delta v}{v} = \frac{v(T) - v(T_0)}{v(T_0)} = C \ln \left[\frac{T}{T_0} \right] \quad \text{with } C = \frac{\bar{P} \gamma_l^2}{\rho v_l^2}, \quad (1)$$

provided that $\hbar\omega \ll kT$ and $P(E) = \bar{P}$ with \bar{P} a constant, the density of states of tunneling systems. The parameter γ_l represents the coupling between the tunneling states and the longitudinal phonons. T_0 is an arbitrary reference temperature. Our very-low temperature observations are in agreement with the predictions of the model. Below 2 K, the velocity increases logarithmically with the temperature and is also frequency independent. The condition $\hbar\omega \ll kT$ of (1) was fulfilled (at the lowest temperatures $\hbar\omega \simeq 0.1 kT$). $T_0 = 0.33$ K is taken as a reference temperature. As can be seen in Fig. 1, the change of the sound velocity is no longer frequency independent above 2 K and deviates from the logarithmic law. This is also observed in glasses and is attributed to the relaxational interaction between the ultrasonic wave and the TS. The tunneling model distinguishes between two different regimes: $\omega\tau_m \gg 1$ and $\omega\tau_m \ll 1$, with τ_m the smallest relaxation time of the TS. At very low temperatures, where the condition $\omega\tau_m \gg 1$ holds, the contribution of the relaxational process is negligible. This is the region discussed above, where the velocity change is attributed to the resonant process only. At higher temperatures, for which $\omega\tau_m \ll 1$, and where the additional velocity change due to the one-phonon relaxation process has to be taken into account, a logarithmic decrease of the velocity is expected with a slope of half that of the resonant part.¹³ This logarithmic decrease was not observed in our case, nor was it detected in high-frequency measurements in glasses. This could be explained by the presence of higher-order phonon relaxational processes, which mask the one-phonon relaxational process in our frequency range.¹⁴

In Fig. 2, a comparison is given between the electron-irradiated sample (E3) and a neutron-irradiated specimen (K9), our lowest neutron dose ($0.85 \times 10^{18} \text{ n/cm}^2$, $E \geq 0.3$ MeV). It is known that the disordering processes for both types of irradiations are quite different. Neutrons cause displacement cascades and it is generally accepted that a 20-Å-diam disordered region is created for each impact.¹⁵ Electrons, on the other hand, because of their small mass, cannot cause secondary displacements and as a result smaller defects are created. It is relevant to inquire whether this leads to different tunneling systems. From our velocity data in Fig. 2, a comparison between the coupling parameters γ can be made. The temperature T_R of the maximum velocity varies as $K_3^{-1/3}$ ($K_3 \sim \gamma^2$).¹⁴ It is clear from Fig. 2 that the coupling constants of the electron-irradiated sample and the neutron-irradiated specimen are similar, in spite of the different disorder processes. As the differences $\Delta v/v$ are extremely small, the temperature of the maximum is not so well defined and small differences in the coupling parameters could therefore not be detected. It is remarkable that electron irradiation, which causes small defects, induces tunneling states similar to those in neutron-irradiated quartz, and therefore also to those in vitreous silica.⁵

From the slope of the resonant part of the velocity

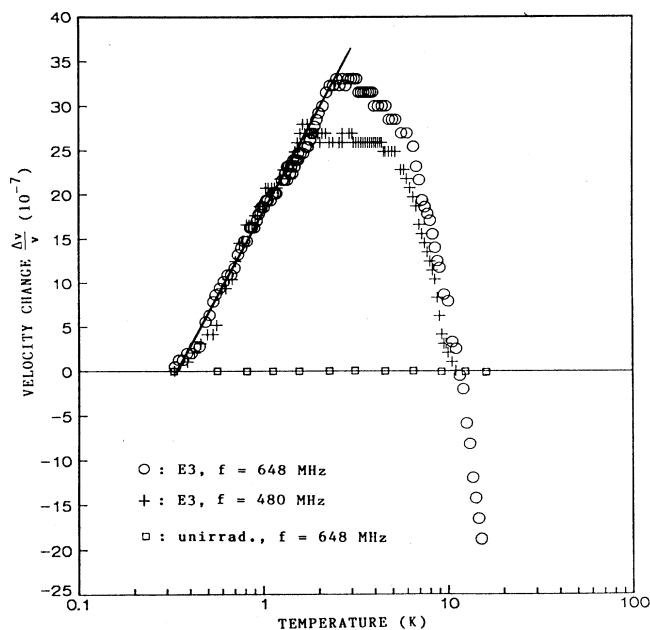


FIG. 1. Velocity change as a function of temperature for electron-irradiated quartz, sample E3 (dose, $1.0 \times 10^{20} \text{ e/cm}^2$; $E = 3$ MeV) for two frequencies, and for unirradiated quartz.

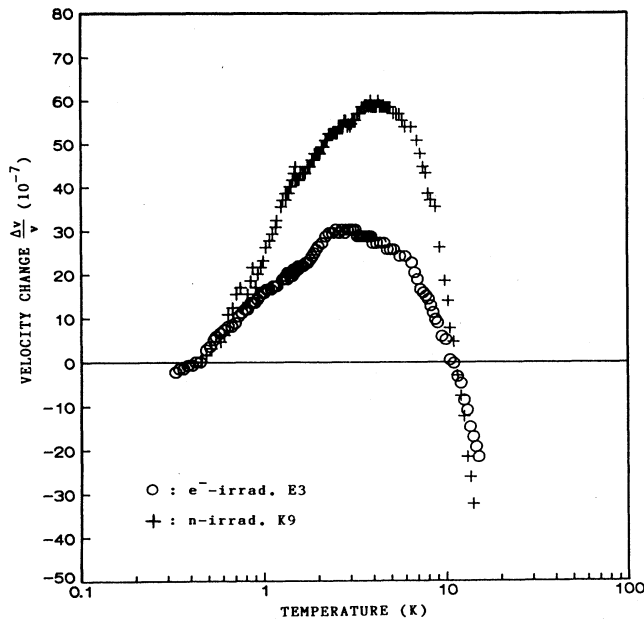


FIG. 2. Velocity change as a function of temperature for electron-irradiated quartz, sample *E3* (dose, $1.0 \times 10^{20} e/cm^2$; $E = 3$ MeV) and for neutron-irradiated quartz, sample *K9* (dose, $0.85 \times 10^{18} n/cm^2$; $E \geq 0.3$ MeV).

change in Figs. 1 and 2, the parameters C and $\bar{P}\gamma_l^2$ of (1) can be deduced. The results for samples *E3* and *K9* are given in Table I, as well as the values for vitreous silica,¹² also deduced from the logarithmic dependence of the velocity. The TS parameters derived from the sound velocity are known to be very reliable, since they can be derived without any additional assumption or parameters and since the logarithmic dependence can be seen over a rather extended temperature interval. The values obtained from our ultrasonic attenuation measurements are also given in the table.⁹ They were deduced from the height of the plateau corresponding to the regime $\omega\tau_m \ll 1$ of the relaxational attenuation. As can be seen in the table, samples *E3* and *K9* differ by a factor of 2.5, while the values for vitreous silica are about 2 orders of magnitude larger. Table I also shows that velocity and attenuation measurements lead to different values for $\bar{P}\gamma_l^2$. This discrepancy has already been observed in many glasses and it was suggested that it is due to the

fact that different tunneling states are probed in the two experiments.¹³ Indeed, in the case of the logarithmic part of the velocity, mainly TS with the smallest relaxation time, τ_m , are probed, whereas at the height of the plateau in the ultrasonic absorption, mainly TS with $\omega\tau = 1$ are involved. It is more appropriate to compare the relative differences between the different samples. Then, as can be seen in Table I, both measurements lead to similar results: $\bar{P}\gamma_l^2$ is a factor of about 2.5 smaller for *E3* than for *K9*, and there is a difference of a factor of about 150 between *E3* and vitreous silica. From these values of $\bar{P}\gamma_l^2$ it also follows that the density of states \bar{P} in *E3* is 2 orders of magnitude smaller than in vitreous silica. We note that a much higher dose is needed, to obtain similar values of $\bar{P}\gamma_l^2$, in the case of electron irradiation, than in neutron-irradiated quartz (see Table I). We shall come back to this point further on.

Let us now go into more detail concerning the damage created by high-energy electrons in quartz. It is generally known that electrons, because of their smaller mass, do not cause displacement cascades, and as a result smaller defects are created than with neutrons. Diffuse x-ray scattering studies performed on one of our samples (*E2*),¹⁶ show that highly disordered extended regions, such as found in neutron-irradiated quartz, are not present. In addition, positron-annihilation lifetime measurements performed on *E2* (Ref. 17), indicate that an amorphous phase is not present, in contrast to neutron-irradiated quartz. On the other hand, EPR studies on sample *E2* indicate that more positional disorder is present than single point defects.¹⁸ The observed E' lines show a broadening which was not observed for lower doses,¹⁹ but which is similar to those in neutron-irradiated quartz.

It is generally known that the main structural damage caused by electron irradiation in solids is the creation of point defects as a consequence of the knock-on process. Semenov *et al.*²⁰ calculated the Frenkel-defect concentration as the result of knock-on damage in quartz caused by 1-MeV electrons and found a concentration of $1.1 \times 10^{14}/cm^3$ for a dose of $10^{14} e/cm^2$. (This means that one Frenkel pair is created for each electron impact.) In quartz, however, as a result of the flexibility of the bonds, the ionizing component of the radiation also seems to have an important impact on the structural damage.^{21,22} From transmission-electron-microscopy (TEM) studies, a radiolytic mechanism has been put forward to account for this damage process.²² According to

TABLE I. TS parameters.

Sample	Dose	C (velocity)	$\bar{P}\gamma_l^2$ (velocity) (g/cm s ²)	$\bar{P}\gamma_l^2$ (attenuation) (g/cm s ²)
e^- irradiated (<i>E3</i>)	$1.0 \times 10^{20} e/cm^2$ ($E = 3$ MeV)	1.6×10^{-6}	1.4×10^6	2.1×10^6
n irradiated (<i>K9</i>)	$0.85 \times 10^{18} n/cm^2$ ($E \geq 0.3$ MeV)	3.7×10^{-6}	3.2×10^6	6.0×10^6
vitreous silica	unirradiated	2.9×10^{-4} ^a	22×10^7 ^a	48×10^7 ^b

^aReference 12.

^bReference 26.

this model, electron irradiation can give rise to excitations of Si—O bonds. The instability of these excited Si—O bonds leads to bond breakage and removal of the oxygen atom. A Si—O—O—Si peroxy linkage can be formed together with an E'' oxygen vacancy. The oxygen vacancy and the peroxy linkage can be considered as a closely spaced Frenkel pair. Frenkel pairs, whether they arise from the knock-on process or from a radiolytic mechanism, increase the freedom of reorientation of SiO_4 tetrahedra and hence can lead to structural damage.²² It is likely that for the dose used, rearrangements of tetrahedra have taken place, possibly involving cooperative effects. We suggest that the TS originate in the regions where these rearrangements have taken place. The presence of large displacement zones, as is the case for neutron-irradiated quartz, does not seem to be a necessary condition for the existence of TS. It is noteworthy that the two disordering processes induce tunneling states of a similar nature. We note, however, that the greater efficiency of neutron irradiation in inducing damage as a result of cascade processes renders the necessary cooperative rotations easier than does stepwise accumulation of Frenkel pairs arising from electron irradiation. This can explain the large difference in the density of states of TS between similar neutron and electron doses: in neutron-irradiated quartz, the density of states of TS is already sa-

turated for a neutron dose of 10^{20} n/cm^2 ,²³ whereas only about 2% of the saturation value is found for our electron-irradiated sample, exposed to a dose of 10^{20} e/cm^2 . Recently, we have argued that the TS in neutron-irradiated quartz might be related to the so-called α_1 - α_2 regions.²³ As a result of neutron irradiation, SiO_4 tetrahedra pass more easily from their original α_1 form to the opposite one, rotated by 180° around the c -axis, the so-called twin-configuration or α_2 form.²⁴ In TEM studies, it was observed that such twinning is also induced by electron irradiation.²⁵ It would be interesting to investigate whether the TS in electron-irradiated quartz could also reside at the boundaries of these twin domains, as we have suggested for neutron-irradiated quartz.²³

ACKNOWLEDGMENTS

The authors thank S. Hunklinger for interesting discussions. They are also grateful to the Belgian Inter-universitair Instituut voor Kernwetenschappen (IIKW) and K. U. Leuven for financial support and to the Centre d'Etudes Nucléaires—Grenoble for the electron irradiations.

¹For a review, see *Amorphous Solids: Low Temperature Properties*, edited by W. A. Phillips (Springer-Verlag, Berlin, 1981).

²P. W. Anderson, B. I. Halperin, and C. M. Varma, *Philos. Mag.* **25**, 1 (1972); W. A. Phillips, *J. Low Temp. Phys.* **7**, 351 (1972).

³S. Hunklinger and W. Arnold, in *Physical Acoustics*, edited by W. P. Mason and R. N. Thurston (Academic, New York, 1976), Vol. 12, p. 155.

⁴C. Laermans, *Phys. Rev. Lett.* **42**, 250 (1979).

⁵B. Golding, J. E. Graebner, W. H. Haemmerle, C. Laermans, *Bull. Am. Phys. Soc.* **24**, 495 (1979); B. Golding and J. E. Graebner, in *Phonon Scattering in Condensed Matter*, edited by H. J. Maris (Plenum, New York, 1980), p. 11.

⁶J. W. Gardner and A. C. Anderson, *Phys. Rev. B* **23**, 474 (1981).

⁷For a recent review, see C. Laermans, in *Structure and Bonding in Non-Crystalline Solids*, edited by G. Walrafen and A. Revesz (Plenum, New York, 1986), p. 325.

⁸C. Laermans, A. M. de Goër, and M. Locatelli, *Phys. Lett.* **80A**, 331 (1980); A. M. de Goër, M. Locatelli, and C. Laermans, *J. Phys. (Paris), Colloq.* **42**, C6-78 (1981).

⁹C. Laermans and A. Vanelstraete, *Phys. Rev. B* **34**, 1405 (1986).

¹⁰C. Laermans and A. Vanelstraete, *Phys. Rev. B* **35**, 6399 (1987).

¹¹R. Truell, C. Elbaum, and B. B. Chick, *Ultrasonic Methods in Solid State Physics* (Academic, New York, 1969).

¹²L. Piché, R. Maynard, S. Hunklinger, and J. Jäckle, *Phys. Rev. Lett.* **32**, 1426 (1974).

¹³A. K. Raychaudhuri and S. Hunklinger, *Z. Phys. B* **57**, 113 (1984).

¹⁴P. Doussineau *et al.*, *J. Phys. (Paris)* **46**, 979 (1985).

¹⁵D. Grasse, O. Kocar, H. Peisl, S. C. Moss, and B. Golding, *Phys. Rev. Lett.* **46**, 261 (1981).

¹⁶D. Grasse, M. Müller, H. Peisl, and C. Laermans, *J. Phys. (Paris), Colloq.* **43**, C9-119 (1982).

¹⁷C. Laermans, Mbungu-Tsumbu, D. Segers, M. Dorikens, L. Dorikens-Vanpraet, and A. Van den Bosch, *J. Phys. C* **17**, 763 (1984).

¹⁸A. Stesmans and R. Weeks (private communication).

¹⁹L. E. Halliburton, B. D. Perlson, R. A. Weeks, J. A. Weil, and M. C. Wintersgill, *Solid State Commun.* **30**, 575 (1979).

²⁰K. P. Semenov and A. A. Fotchenkov, *Kristallografiya* **22**, 571 (1977) [*Sov. Phys. Crystallogr.* **22**, 326 (1977)].

²¹Gopal Das and T. E. Mitchell, *Radiat. Eff.* **23**, 49 (1974).

²²L. W. Hobbs and M. R. Pascucci, *J. Phys. (Paris), Colloq.* **41**, C6-237 (1980).

²³A. Vanelstraete and C. Laermans, *Phys. Rev. B* **38**, 6312 (1988).

²⁴R. Comes, M. Lambert, and A. Guiner, in *Interaction of Radiation with Solids*, edited by A. Bishay (Plenum, New York, 1967), p. 319.

²⁵J. J. Comer, *J. Cryst. Growth* **15**, 179 (1972).

²⁶U. Batell, Ph.D. thesis, University of Heidelberg, 1984.